2012 IEEE International Conference on Robotics and Automation
RiverCentre, Saint Paul, Minnesota, USA
May 14-18, 2012

Robot End-effector Sensing with Position Sensitive Detector and Inertial Sensors*

Cong Wang, Wenjie Chen, and Masayoshi Tomizuka

Abstract— **For the motion control of industrial robots, the end-effector performance is of the ultimate interest. However, industrial robots are generally only equipped with motor-side encoders. Accurate estimation of the end-effector position and velocity is thus difficult due to complex joint dynamics. To overcome this problem, this paper presents an optical sensor based on position sensitive detector (PSD), referred as PSD camera, for direct end-effector position sensing. PSD features high precision and fast response while being cost-effective, thus is favorable for real-time feedback applications. In addition, to acquire good velocity estimation, a kinematic Kalman filter (KKF) is applied to fuse the measurement from the PSD camera with that from inertial sensors mounted on the end-effector. The performance of the developed PSD camera and the application of the KKF sensor fusion scheme have been validated through experiments on an industrial robot.**

I. INTRODUCTION

In many applications of industrial robots, the primary objective is to control the end-effector to track desired trajectories or move to the target positions quickly and accurately. Accurate information of the end-effector position and velocity is important to achieve this objective. Joints of typical industrial robots are driven by motors with gear reducers, and are equipped with motor-side encoders only. Accurate estimation of the end-effector position and velocity is thus difficult due to flexibility, friction, and backlash in the gearing mechanism. To overcome this difficulty, the idea of adopting end-effector sensors has been suggested. Specifically, the capability of measuring the end-effector position directly without physical contact is desirable. In addition, the application of inertial sensors on the end-effector sensing can provide supplemental measurements to achieve good velocity estimation [1].

Desirable features for end-effector position sensing are *non-contact* and *direct*. *Non-contact* excludes any physical contact between the target and the sensor that may intertwine with the workpieces and the tools during the actual robot operation. *Direct* means the target position information should be acquired directly instead of being inferred based on the robot model. Various candidate technologies exist, ranging from laser trackers to ultrasonic range finders ([2], [3], [4], [5]). Despite the broad variety, candidates for non-contact direct position measurement share two common features: a) all methods use light, sound, or radio waves; b) all methods use waves in one of the three ways, i.e., interferometry, time-of-flight (TOF), or projection (checking the position of the wave's focused projection on a sensing plane).

Generally, the measurement precision is limited by the wavelength. For a desired precision at 0.1mm level in industrial robot applications, light waves will be necessary. Among the three ways to utilize waves, interferometry can achieve extremely high precision up to the nano scale, but is also expensive. TOF is most attractive in terms of cost, but can hardly give precision beyond the centimeter level. In terms of cost and precision, projection provides the best balance. A straightforward choice combining light wave and projection may be vision camera in view that the advances of image processing algorithms can make vision systems capable of handling highly intelligent tasks. The slow response and large time latency, however, make it challenge to utilize vision cameras in the feedback loop for real-time motion control. This motivates to find alternatives for image sensors, featuring faster response and higher sampling rate while being cost-effective. Position sensitive detector (PSD) is such an option. In this paper, a camera-like position sensing device, referred as PSD camera, is proposed. It senses the position of infrared markers attached to targets such as the robot end-effector with promising accuracy and precision. It also provides a much faster response than typical vision cameras, and can be sampled at a much higher sampling rate.

It turns out that, however, the position measurement from the PSD camera alone is not sufficient to provide good velocity information. To overcome this limitation, additional sensors (e.g., inertial sensors) can be installed on the robot end-effector. With proper sensor fusion algorithms, it is possible to obtain good velocity estimation by fusing the measurement from the PSD camera with that from the inertial sensors. KKF, the Kalman filter based on kinematic model, can be a favorable option. It avoids using complex dynamics model and does not require parameters of system dynamics. KKF was originally applied to one-dimensional positioning systems, where the measurements from accelerometer and encoder were fused to provide good velocity estimation ([6], [7], [8]). Recently it has been extended to the three-dimensional case, where the angular velocity measurement from Gyroscope has been utilized to capture the rotational motion [1].

The remainder of this paper is organized as follows. Section II presents the development of the PSD camera for end-effector position sensing. Investigation on noise mitigation and calibration, as well as the performance tests, is discussed. Section III presents the application of KKF to fuse the measurements from the PSD camera and inertial sensors

*This work was supported by FANUC Ltd.

C. Wang, W. Chen, and M. Tomizuka are with the Department of Mechanical Engineering, University of California, Berkeley, CA 94720, USA {wangcong,wjchen,tomizuka}@berkeley.edu

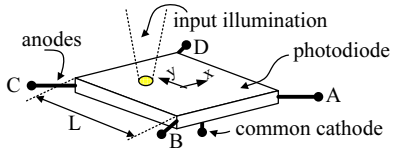

Fig. 1. Two-dimensional lateral effect PSD

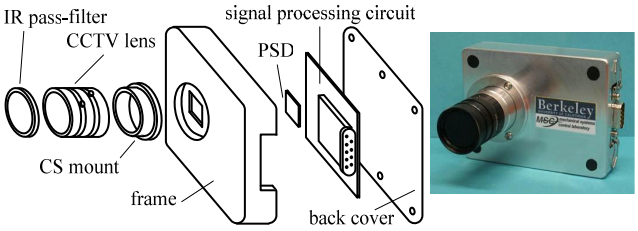

Fig. 2. Structure of the PSD camera prototype

for the estimation of end-effector velocity. Experimental validation is conducted on an industrial robot. The conclusion is given in Section IV.

II. PSD CAMERA FOR END-EFFECTOR POSITION SENSING

A. Position Sensitive Detector

Position sensitive detector (PSD), unlike CCD/CMOS image sensors which sense input light in image form, senses only the position of a light spot. There are generally two types of PSD, quadrant detector and lateral effect detector. The latter is chosen due to its superiority on effective sensing area. As shown in Fig. 1, the sensing plane of a two-dimensional lateral effect PSD consists of one single piece of photodiode with four anodes and a common cathode. When illuminated, the current generated by photo-electro effect will go through the anodes, with each channel's magnitude proportional to the magnitude of input illumination and the distance between the illuminated area and the anode. The relationship between the current magnitudes and the illumination position is

$$\frac{2x}{L} = \frac{I_A + I_D - I_B - I_C}{I_A + I_B + I_C + I_D}, \frac{2y}{L} = \frac{I_C + I_D - I_A - I_B}{I_A + I_B + I_C + I_D} \quad (1)$$

where $I_\bullet$ is the current through the corresponding anode. x and y are the illumination position on the sensing plane. L is the side length of the effective sensing area.

PSD has a long history of application on laser beam alignment. It has recently been adopted for spatial position sensing in entertainment applications. A successful example is the Wii game system by Nintendo, which equips a PSD at the front of the handheld controller. The illumination from the infrared LED lights located on the Sensor Bar of the Wii system is focused onto the sensing plane of the PSD by a pinhole structure. By sensing the position of the input illumination, the spatial position of the handheld controller can be determined. Inspired by the Wii system, PSD can be used in industrial applications for position sensing by focusing the light from the markers attached to the target onto the sensing plane of PSD with a lens. This forms a PSD camera (Fig. 2). The marker used can either be a retro-reflective one which reflects illumination from a light source, or an active beacon which emits light diffusively. Multiple markers can be sensed by a single PSD camera using multiplexing techniques.

Several advantages make PSD suitable for real-time feedback applications. First, it can achieve a response time at the level of microseconds. Even with the signal processing circuit, a level of 30μs can be expected. This is much faster than that of typical vision cameras, which is generally at the level of milliseconds due to the time for exposure and image processing. In addition, the simple analogue output of PSD can be sampled easily by data acquisition devices with a high sampling rate. Moreover, the PSD camera provides high resolution[1], up to the level of $< 1\mu$m when the sensing plane is 10mm$\times$10mm large. Even under the influence of weak input, poor focusing, and noise, a resolution of 1.5μm can be easily achieved. This corresponds to a precision of 0.15mm for a 500mm$\times$500mm measurement area. In addition, PSD is robust to focusing quality as it still measures the mass center of the illuminated area if the input is not focused. Furthermore, the peak spectral response of most PSD is around infrared. This makes it easy to remove the influence of environmental illumination by using an infrared pass filter. On the other hand, the sole drawback of PSD is the incapability of capturing images as what vision cameras do, and thus is incapable of sensing without marker. However, even for vision cameras, it is also a common practice to use markers of special features that are easy to identify by the image processing algorithms to expedite the response.

B. PSD Camera Design

Fig. 2 shows the structure of the proposed PSD camera. A 9mm$\times$9mm PSD (Hamamatsu, S5991-01) is adopted. It features a 2μs response time, and a typical 1.5μm resolution. A CCTV lens (FUJINON, HF9HA-1B) with 9mm fixed focal length is used. The lens offers a 48°$\times$48° angle-of-view, or a 450mm$\times$450mm field-of-view when the measurement plane locates 500mm in front of the camera. As PSD is robust to focusing quality, the focus adjustment does not matter much. The iris adjustment affects the intensity of total input illumination, and thus the signal-to-noise ratio and measurement precision. A maximum iris (F16) is selected in the experiments. An infrared pass filter (Anchor Optics, CR-39) is used to cut off all the input illumination except that from the markers.

The raw output signals of the PSD are weak current signals, whereas the final output of the PSD camera is the two-dimensional position of the input light spot on the sensing plane of the PSD, represented by two analogue voltage signals ranging from -10V to +10V. A signal processing circuit is used for the conversion. An amplification unit first

[1]Here as the analog resolution, i.e., the minimum position difference that can be distinguished on the sensing plane, equals to half of the sensing precision, and heavily depends on the signal to noise ratio.

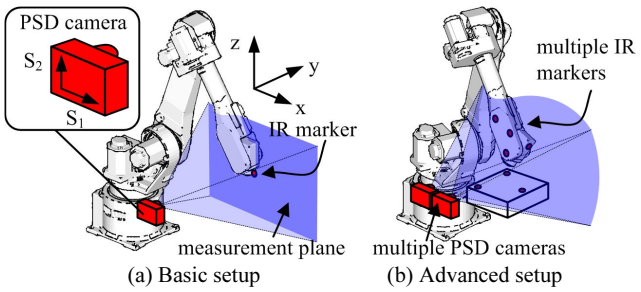

Fig. 3. Setup examples of PSD camera

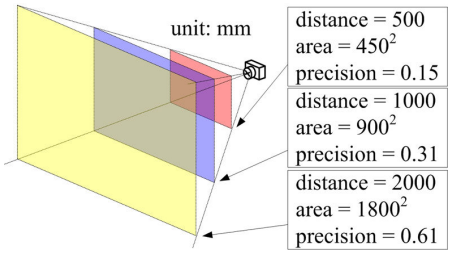

Fig. 4. Precision levels for measurement planes at different distances

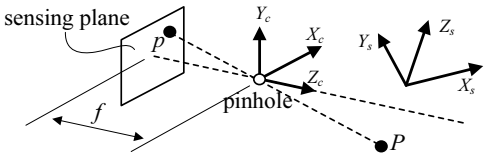

Fig. 5. Ideal perspective projection in a pinhole camera model

transforms the weak current signals to voltage signals, which will then be operated by the addition/subtraction and dividing units to perform the computation of (1). All operations are conducted by analog circuits (i.e., operational amplifiers and analog dividers) instead of digital processor after A/D conversion. This is to prevent the rounding error of the A/D process from being amplified. The output signals of the PSD camera are sampled by a data acquisition device (National Instruments, NI-6023E).

In the basic application setup (Fig. 3 (a)), the PSD camera is set on the ground, with an infrared LED beacon (Vishay, TSAL6400) mounted on the robot end-effector. With the end-effector's trajectory constrained in a plane, this setup provides two-dimensional measurement of the end-effector position. Advanced setup can be configured to achieve more measurement dimensions by using more markers and/or more PSD cameras (Fig. 3 (b)). The PSD camera can also be mounted on the end-effector, while the markers are mounted on the target.

C. Sensing Noise Mitigation and Calibration

In order to achieve both good accuracy and precision, noise mitigation and calibration are necessary for the PSD camera. Precision depends mainly on the sensing noise level, while accuracy depends on calibration. In the actual application on the industrial robot, the PSD camera suffers from strong environmental electro-magnetic interference due to the power supply of the robot servos. In our experiments, the raw output is contaminated by noise with a distribution width of 15mV, which corresponds to a 0.34mm precision when the measurement area is 450mm×450mm large. Shielded twisted pair cable with ferrite beads is used to remove the common-mode noise and suppress the high frequency noise. A digital low-pass filter is also adopted after the A/D process. The filtering phase lag can be sufficiently small if the initial sampling rate is high enough (e.g. ten times of the desired sampling rate). The distribution width of the noise is then reduced to 6.8mV. The corresponding precision levels on the measurement planes located at different distances in front of the PSD camera are summarized in Fig. 4.

Compared to noise mitigation, more effort is needed for calibration. Two types of transformation are involved in the mapping between the spatial position of the target and the output signals of the PSD camera. They correspond to two parts of calibration. The first part, referred as linear calibration, corresponds to the perspective projection relationship in an ideal pinhole camera model (Fig. 5), in which the spatial position of the marker and the position of the projected light spot on the sensing plane of PSD are related by

$$x_c = \frac{f}{Z_c} X_c, \qquad y_c = \frac{f}{Z_c} Y_c \tag{2}$$

$$\begin{bmatrix} X_c & Y_c & Z_c \end{bmatrix}^{\mathrm{T}} = \boldsymbol{R}\left(\begin{bmatrix} X_s & Y_s & Z_s \end{bmatrix}^{\mathrm{T}} - \boldsymbol{T} \right) \tag{3}$$

where $(X_\bullet, Y_\bullet, Z_\bullet)$ and $(x_\bullet, y_\bullet, z_\bullet)$ denote positions of the marker P and its projection p respectively. The subscript c indicates the camera fixed coordinates, while s indicates the workspace coordinates of the robot. $\boldsymbol{R}$ and $\boldsymbol{T}$ are the rotation matrix and translation vector between the two coordinate systems. The camera outputs are thus $S_1 = K_1 x_c$ and $S_2 = K_2 y_c$, where K_1 and K_2 are the sensitivity gains of the PSD along its two axes. After the PSD camera is installed, linear calibration is conducted to determine K_1, K_2, $\boldsymbol{R}$, and $\boldsymbol{T}$. This is accomplished by measuring several points in the measurement plane by both the PSD camera and a reference instrument, then applying a least-squares fitting.

Besides linear calibration, a nonlinear calibration process is also necessary. It is to compensate the nonlinear distortion in the overall sensing system, including the optical distortion of the lens, and the nonlinear response of the PSD and the signal processing circuit. Without considering these, it is very difficult to achieve an accuracy better than 2mm for a 450mm×450mm measurement area in our experiments. The common practice for nonlinear calibration is to model distortion with analytical models, which usually involve higher order polynomials [9], [10]. Such models, however, can only provide a rough approximation of the actual nonlinearity. The resulting accuracy of the PSD camera is still unacceptable. As an alternative, the distortion is recorded by a lookup table built by densely scanning the sensing area point by point. The true values (obtained from a reference instrument) of every point and their corresponding PSD camera measurements

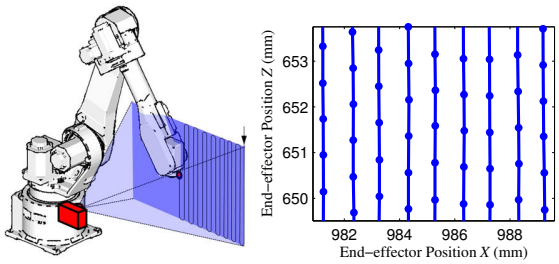

Fig. 6. Sensing area scanning for PSD nonlinear calibration

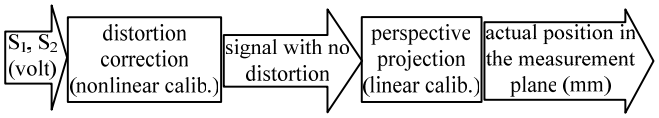

Fig. 7. PSD camera calibration

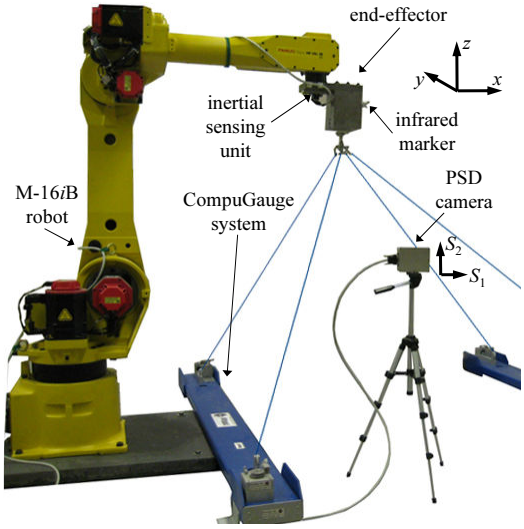

Fig. 8. Experimental setup for performance tests

(contaminated by distortion) are recorded and stored in the lookup table. Building such a lookup table can be time consuming. However, it needs to be conducted only once since the nonlinearity is the intrinsic characteristic of the PSD camera.

In the experimental setup for calibration, the measurement plane is located parallel to the PSD sensing plane, 500mm in front of the PSD camera. An infrared marker is attached to the end-effector of an industrial robot (FANUC, M-16*i*B), which is used to move the marker to specified locations in the measurement plane. Meanwhile, the CompuGauge system developed by Dynalog is used as a reference instrument. Its measurement of the end-effector position is regarded as the true value. CompuGauge senses the motion of the end-effector by measuring the motion of four strings attached to the end-effector. It gives a precision of 0.01mm, and is widely used for robot calibration.

As shown in Fig. 6, during the scanning, the end-effector moves through the sensing area line by line without stop. The gap between adjacent lines is 1mm. Points are sampled along the lines with a time step corresponding to 1mm displacement. The actual path of the end-effector, however, will not be exactly the same as programmed. The sampled points are thus not uniformly aligned. This brings difficulty to the interpolation in the table lookup process. The problem is usually termed as scattered data interpolation [11]. One common step of various algorithms is to find the neighboring points around the inquired point. This induces significant computation load which is undesirable for real-time feedback applications. Thus, an alternative method is used. A new lookup table is built with ideally aligned grid. The value of each point on the grid is obtained by interpolation from the original table with the non-uniform grid. Any scattered data interpolation algorithm may be used. The result does not vary much as the grid is dense. This work needs to be done only once during the nonlinear calibration. The new lookup table can then be interpolated easily in real-time during the actual sensing process.

As illustrated in Fig. 7, in the actual operations of the PSD camera, the measured signals are first corrected to compensate distortion using the lookup table built in advance during the nonlinear calibration, then transformed through the perspective projection model. The final result represents the actual position of the target in the measurement plane.

D. Performance Tests

Tests are conducted to evaluate the performance of the PSD camera for end-effector position sensing. The basic single-marker-single-camera configuration is adopted (Fig. 3 (a)). The measurement plane locates 500mm away from the PSD camera. The end-effector of the robot (FANUC, M-16*i*B) is programmed to move along square and circle paths without orientation change. The end-effector position is measured by both the PSD camera and the CompuGauge system (Fig. 8), with the measurement from the latter regarded as the true value.

Fig. 9 shows the comparison of the measurement results. The figures on the right column show the zoomed-in details of the figures on the left. Among repetitive experiments, an average accuracy[2] at the level of 0.05∼0.1mm is achieved, which is quite promising considering the size of the measurement area (450mm×450mm). Higher accuracy can be achieved if a smaller measurement area is used.

III. END-EFFECTOR VELOCITY ESTIMATION WITH PSD CAMERA AND INERTIAL SENSORS

In general, both position and velocity information of the end-effector are important for motion control. The developed PSD camera has good capability on position sensing. Its measurement alone, however, is not sufficient to support fine velocity estimation. As shown in Fig. 11, the velocity estimation acquired by differentiating the PSD measurement is

[2]Represented by the root-mean-square difference between the measurements from the PSD camera and CompuGauge system.

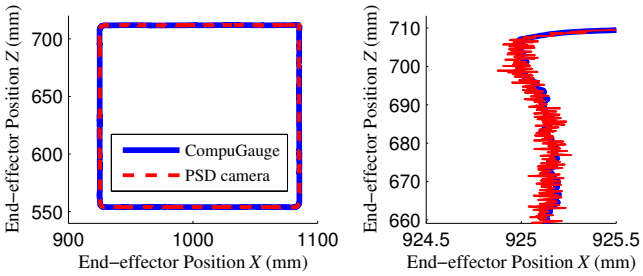

(a) Square path

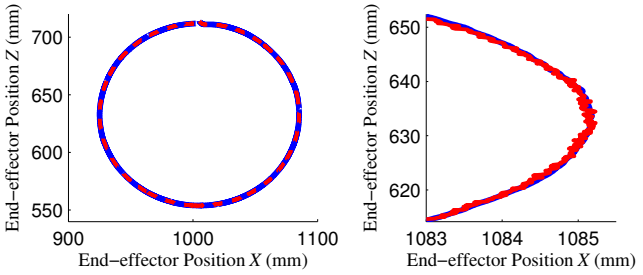

(b) Circle path

Fig. 9. Measurement comparison between PSD camera and CompuGauge

highly unacceptable. Methods have been studied to improve velocity estimation acquired from position measurement. Most of them, however, are based on dynamics models[8]. They require accurate parameters of system dynamics, and are difficult to apply due to the complexity of robot dynamics. One promising alternative is to use a sensor fusion algorithm to include measurements from additional inertial sensors (accelerometer and gyroscope) installed on the target (e.g. robot end-effector). No parameter of system dynamics is needed if the kinematic model is used to relate position to acceleration and angular velocity, where the latter two are treated as the model input and measured directly by accelerometer and gyroscope. This is the basic idea of kinematic Kalman filter (KKF). Here, a KKF for three-dimensional rigid body motion [1] is formulated to fuse the measurements from the PSD camera and inertial sensors.

A. KKF for 3D Rigid Body Motion

The kinematic model of robot end-effector can be described as

$$\dot{\boldsymbol{p}}^s_{TCP} = \boldsymbol{v}^s_{wr} + \boldsymbol{R}[\boldsymbol{\omega}^b\times]\boldsymbol{r}^b_{TCP/wr} \quad (4)$$

$$\dot{\boldsymbol{v}}^s_{wr} = \boldsymbol{R}\boldsymbol{f}^b_{wr} + \boldsymbol{g}^s \quad (5)$$

$$\dot{\boldsymbol{R}} = \boldsymbol{R}[\boldsymbol{\omega}^b\times] \quad (6)$$

where the subscript TCP indicates tool center point, and wr indicates the wrist point where the inertial sensors locate. s and b denote the workspace coordinates of the robot and the body coordinates of the end-effector respectively. $\boldsymbol{p}$ is position, $\boldsymbol{v}$ is velocity, $\boldsymbol{\omega}$ is angular velocity, $\boldsymbol{f}$ is acceleration, $\boldsymbol{g}$ is gravity, and $\boldsymbol{R}$ is the rotation matrix of the end-effector. $[\bullet\times] \in \mathbb{R}^{3\times3}$ is the skew-symmetric matrix, equivalent to the cross product operation of the corresponding vector. With this model, at the k-th time step, the open loop prediction can be conducted as

$$\begin{aligned}\hat{\boldsymbol{R}}(k+1|k) = \hat{\boldsymbol{R}}(k|k)(\boldsymbol{I} + T[\bar{\boldsymbol{\omega}}^b(k+1)\times] \\ +\frac{T^2}{2}[\bar{\boldsymbol{\omega}}^b(k+1)\times]^2)\end{aligned} \quad (7)$$

$$\begin{aligned}\begin{bmatrix}\hat{\boldsymbol{p}}^s_{TCP}(k+1|k)\\ \hat{\boldsymbol{v}}^s_{wr}(k+1|k)\end{bmatrix} = \begin{bmatrix}\boldsymbol{I} & T\boldsymbol{I}\\ 0 & \boldsymbol{I}\end{bmatrix}\begin{bmatrix}\hat{\boldsymbol{p}}^s_{TCP}(k|k)\\ \hat{\boldsymbol{v}}^s_{wr}(k|k)\end{bmatrix} \\ +T\begin{bmatrix}-\hat{\boldsymbol{R}}(k+1|k)[\boldsymbol{r}^b_{TCP/wr}\times] & \frac{T}{2}\hat{\boldsymbol{R}}(k+1|k)\\ \boldsymbol{0} & \hat{\boldsymbol{R}}(k+1|k)\end{bmatrix} \\ \times\begin{bmatrix}\bar{\boldsymbol{\omega}}^b(k+1)\\ \bar{\boldsymbol{f}}^b_{wr}(k+1)\end{bmatrix} + T\begin{bmatrix}\frac{T}{2}\boldsymbol{I}\\ \boldsymbol{I}\end{bmatrix}\hat{\boldsymbol{g}}^s\end{aligned} \quad (8)$$

where $\hat{\bullet}$ indicates estimated value, $\bar{\bullet}$ indicates measured value. T is the sampling time. The position measurement ($\bar{\boldsymbol{p}}^s_{TCP}$) from the PSD camera is then used to perform correction as follows

$$\begin{aligned}\delta\hat{\boldsymbol{x}}(k+1|k+1) = \delta\hat{\boldsymbol{x}}(k+1|k) + \boldsymbol{L}(k+1) \\ \cdot[\bar{\boldsymbol{p}}^s_{TCP}(k+1) - \hat{\boldsymbol{p}}^s_{TCP}(k+1|k) + \delta\hat{\boldsymbol{p}}(k+1|k)]\end{aligned} \quad (9)$$

where $\delta\hat{\boldsymbol{x}} = \begin{bmatrix}\delta\hat{\boldsymbol{p}}^T & \delta\hat{\boldsymbol{v}}^T & \hat{\boldsymbol{\psi}}^T\end{bmatrix}^T$ includes the correction terms for position, velocity, and rotation matrix. $\boldsymbol{L}$ is the Kalman filter gain determined from the estimation error propagation. Detailed derivation can be found in [1].

B. Experimental Results

Experimental validation is conducted on a FANUC M-16*i*B industrial robot. The hardware setup is the same as that in Section II-D. An inertial measurement unit (Analog Devices, ADIS16400) is installed on the end-effector (Fig. 8). It includes a triaxial gyroscope and a triaxial accelerometer. Again, the TCP position of the end-effector is measured by both the PSD camera and the CompuGauge system. The measurement from the latter and its differentiation are regarded as the true position and velocity. The sampling time is set as 1ms. Two sets of experiments are conducted. In the first set, one marker is installed on the end-effector, providing two-dimensional sensing of position without rotation measurement. The trajectories used are the same with those in the PSD camera performance tests (Fig. 9). Fig. 11(a) and Fig. 11(b) show the velocity estimation results using KKF, as well as a comparison with the results generated by differentiation of the position measurement from the PSD camera. The superiority of the sensor fusion scheme is evident.

In the second set of experiments, two markers are installed on the end-effector (Fig. 10), with a 120mm distance between them. The motion of the end-effector is still constrained in the x-z plane, with orientation change allowed only along the y axis. With two markers, the TCP position can be determined by triangulation based on the measured positions of the markers and their known locations on the end-effector. The markers are controlled by a micro-processor (Atmel, Mega328) to flash alternately, and thus sensed by the PSD camera alternately. The end-effector path is illustrated in Fig. 10. Fig. 11(c) shows the velocity estimation result.

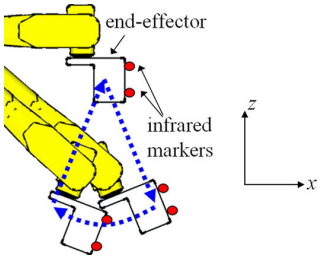

Fig. 10. End-effector path with orientation change

Again, the result from KKF shows significant superiority. However, compared with the first set of experiments where no orientation change is involved, the velocity estimation along the z axis shows some drifting phenomena. This is due to the calibration inaccuracy of the gyroscope. To address this, a more complicated sensor fusion algorithm with the consideration of sensor self-calibration may be necessary.

IV. CONCLUSIONS AND FUTURE WORK

The non-contact direct measurement of end-effector position and good estimation of its velocity are highly desirable to overcome the limitations of conventional indirect drive servo system of industrial robots. This paper first proposed the development of a PSD camera using position sensitive detector. While being cost-effective, the PSD camera provides much faster response than typical vision systems. With proper work on noise mitigation and calibration, the PSD camera has demonstrated promising precision and accuracy. These advantages make it favorable to be utilized in real-time feedback systems.

Furthermore, to acquire good velocity estimation, a kinematic Kalman filter based on a three-dimensional rigid body motion model has been applied to perform sensor fusion, where the measurements from inertial sensors mounted on the robot end-effector have been fused with that from the PSD camera. Performance tests of the PSD camera and validation experiments of the sensor fusion scheme were conducted on a FANUC M-16*i*B robot. Promising results have been demonstrated on both position sensing and velocity estimation of the robot end-effector.

Future work will be conducted on increasing the measurement dimensions of the PSD camera system by using more markers and/or more than one camera. Particularly, with more markers, advanced multiplexing technique may be required. In addition, self-calibration techniques of inertial sensors to incorporate with the KKF scheme may be a key aspect if the velocity estimation is to be further improved.

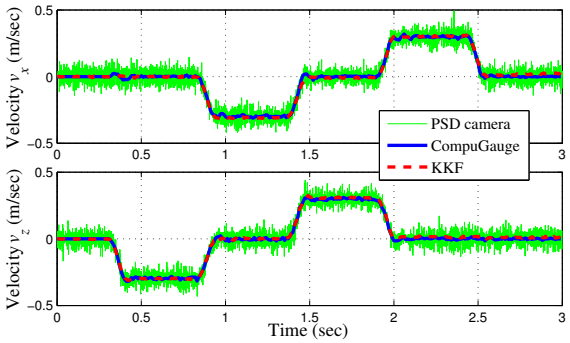

(a) Square path with no orientation change

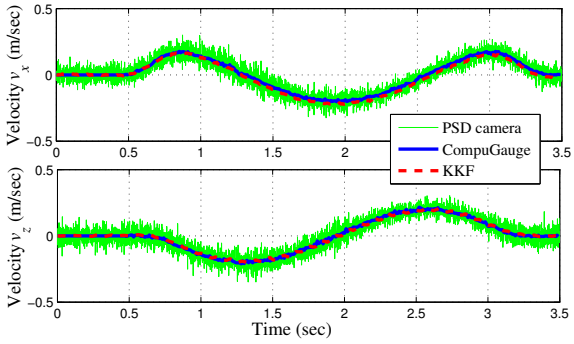

(b) Circle path with no orientation change

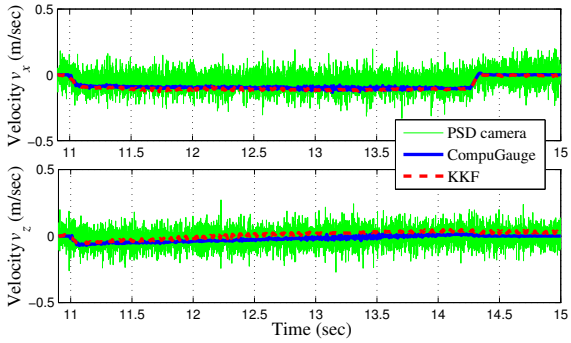

(c) Curve path with orientation change

Fig. 11. TCP velocity estimation results

REFERENCES

[1] S. Jeon, M. Tomizuka, and T. Katou, "Kinematic Kalman filter (KKF) for robot end-effector sensing," *Journal of Dynamic Systems, Measurement, and Control*, vol. 131, no. 2, pp. 21010–21018, 2009.

[2] G. Brooker, *Introduction to Sensors for Ranging and Imaging*. Scitech, 2009.

[3] K. Peiponen, R. Myllyla, and A. V. Priezzhev, *Optical Measurement Techniques*. Springer, 2009.

[4] F. Blais, "Review of 20 years of range sensor development," *Journal of Electronic Imaging*, vol. 13, pp. 231–240, Jan. 2004.

[5] B. Shirinzadeh, P. L. Teoh, Y. Tian, M. M. Dalvand, Y. Zhong, and H. C. Liaw, "Laser interferometry-based guidance methodology for high precision positioning of mechanisms and robots," *Robotics and Computer-Integrated Manufacturing*, vol. 26, pp. 74–82, Feb. 2010.

[6] H. C. Shim, M. Kochem, and M. Tomizuka, "Use of accelerometer for precision motion control of linear motor driven positioning system," in *Proceedings of the 24th Annual Conference of the IEEE Industrial Electronics Society*, vol. 4, pp. 2409–2414, Aachen, Germany, 1998.

[7] D. J. Lee and M. Tomizuka, "State/parameter/disturbance estimation with an accelerometer in precision motion control of a linear motor," in *Proceedings of ASME IMECE'01*, DSC-2457, New York, 2001.

[8] S. Jeon and M. Tomizuka, "Benefits of acceleration measurements in velocity estimation and motion control," *Control Eng. Pract.*, vol. 15, no. 3, pp. 325–332, 2007.

[9] B. Cyganek and J. P. Siebert, *An Introduction to 3D Computer Vision Techniques and Algorithms*. WILEY, 2009.

[10] J. Pers and S. Kovacic, "Nonparametric, model-based radial lens distortion correction using tilted camera assumption," in *Proceedings of the Computer Vision Winter Workshop*, pp. 286–295, Citeseer, 2002.

[11] I. Amidror, "Scattered data interpolation methods for electronic imaging systems: a survey," *J. Electron. Imaging*, vol. 11, no. 2, pp. 157–176, 2002.